

AD-A200 842

DTIC FILE COPY ②

OFFICE OF NAVAL RESEARCH

Contract N00014-83-K-0470-P00003

R&T Code NR 33359-718

Technical Report No. 106

Mathematical Modelling of Transport through Conducting Polymer Films.
I. The Poly(paraphenylene) System

by

K. Ashley, S. Pons and M. Fleischmann

Prepared for publication in J. Electroanal. Chem.

Department of Chemistry
University of Utah
Salt Lake City, UT 84112

July 15, 1988

DTIC
ELECTE
NOV 14 1988
S & E D

Reproduction in whole, or in part, is permitted for
any purpose of the United States Government

This document has been approved
for public release and sales in
distribution is unlimited.

88 11 10 087

SECURITY CLASSIFICATION OF THIS PAGE

REPORT DOCUMENTATION PAGE

1a. REPORT SECURITY CLASSIFICATION Unclassified			1b. RESTRICTIVE MARKINGS	
2a. SECURITY CLASSIFICATION AUTHORITY			3. DISTRIBUTION / AVAILABILITY OF REPORT Approved for public release and sale. Distribution unlimited.	
2b. DECLASSIFICATION / DOWNGRADING SCHEDULE				
4. PERFORMING ORGANIZATION REPORT NUMBER(S) ONR Technical Report No. 106			5. MONITORING ORGANIZATION REPORT NUMBER(S)	
6a. NAME OF PERFORMING ORGANIZATION University of Utah		6b. OFFICE SYMBOL (if applicable)	7a. NAME OF MONITORING ORGANIZATION	
6c. ADDRESS (City, State, and ZIP Code) Department of Chemistry Henry Eyring Building Salt Lake City, UT 84112			7b. ADDRESS (City, State, and ZIP Code)	
8a. NAME OF FUNDING / SPONSORING ORGANIZATION Office of Naval Research		8b. OFFICE SYMBOL (if applicable)	9. PROCUREMENT INSTRUMENT IDENTIFICATION NUMBER N00014-83-K-0470-P00003	
8c. ADDRESS (City, State, and ZIP Code) Chemistry Program, Code 1113 800 N. Quincy Street Arlington, VA 22217			10. SOURCE OF FUNDING NUMBERS	
			PROGRAM ELEMENT NO.	PROJECT NO.
			TASK NO.	WORK UNIT ACCESSION NO.
11. TITLE (Include Security Classification) Mathematical Modelling of Transport through Conducting Polymer Films. I. The Poly(paraphenylene) System				
12. PERSONAL AUTHOR(S) K. Ashley, S. Pons and M. Fleischmann				
13a. TYPE OF REPORT Technical		13b. TIME COVERED FROM 9/87 TO 7/88	14. DATE OF REPORT (Year, Month, Day) July 15, 1988	
15. PAGE COUNT 24				
16. SUPPLEMENTARY NOTATION				
17. COSATI CODES			18. SUBJECT TERMS (Continue on reverse if necessary and identify by block number) conducting polymers, transport	
FIELD	GROUP	SUB-GROUP		
19. ABSTRACT (Continue on reverse if necessary and identify by block number) Attached.				
20. DISTRIBUTION / AVAILABILITY OF ABSTRACT <input checked="" type="checkbox"/> UNCLASSIFIED / UNLIMITED <input type="checkbox"/> SAME AS RPT <input type="checkbox"/> DTIC USERS			21. ABSTRACT SECURITY CLASSIFICATION Unclassified	
22a. NAME OF RESPONSIBLE INDIVIDUAL Stanley Pons			22b. TELEPHONE (Include Area Code) (801)581-4760	22c. OFFICE SYMBOL

Abstract

Chronoamperometric data obtained from doped poly(paraphenylene)-modified electrodes (electroformed from biphenyl) are predicted using a migration-diffusion transport model. The experimental response to a double potential step is dependent on the nature of the supporting electrolyte which is present during polymer electrodeposition.

Accession For	
NTIS GRA&I	<input checked="checked" type="checkbox"/>
DTIC TAB	<input type="checkbox"/>
Unannounced	<input type="checkbox"/>
Justification	
By _____	
Distribution/	
Availability Codes	
Dist	Avail. and/or Special
A-1	



MATHEMATICAL MODELING OF TRANSPORT
THROUGH CONDUCTIVE POLYMER FILMS

II. THE POLY(PARAPHENYLENE) SYSTEM

Kevin Ashley

Department of Chemistry
San Jose State University
San Jose, California 95192 USA

Stanley Pons*

Department of Chemistry
University of Utah
Salt Lake City, UT 84112 USA

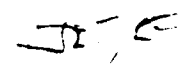
and

Martin Fleischmann

Department of Chemistry
The University
Southampton SO9 5NH UK

*To whom correspondence should be addressed

Introduction

Modeling studies concerning charge transport through organically conductive polymer systems have focussed principally on poly(acetylene) (PA) and poly(pyrrole) (PP) [1-3], with charge transport presumed to occur via polarons, bipolarons, or charged solitons, depending on the system. Apart from theoretical studies on organic conducting polymers, a significant amount of theoretical work has been done in efforts to explain transport phenomena in electrodes modified with inorganic conducting systems such as poly(vinylferrocene) (PVC) and other transition metal-containing polymers [4-7]. To date these theoretical models have been for the most part quantum mechanical in nature, with transport presumed to occur via an electron hopping mechanism. 

Recently workers in the inorganic conducting polymer field have taken diffusion [8-12] and migration [13, 14] of electrolyte material within the polymer matrix into account, and so have begun to treat the problem of transport through polymer films in a more macroscopic fashion. However, a completely macrohomogeneous approach (which includes migrational contributions) to the study of charge transport in conductive polymer systems has to date been realized by only a few workers [15-17]. This modelling scheme, originally developed to describe charge transport processes in porous battery materials [18-22], has been extended to describe the transient current response of electrodes modified with poly($\text{Ru}^{\text{II}}[\text{bipy}]_2[4\text{-vpy}]_2\text{PF}_6^-$) [16]. A theoretical formalism was developed in ref. [17] in an effort to describe the transient current behavior of an organically conducting polymer such as poly(paraphenylene) (PPP). This theoretical development includes diffusional and migrational contributions to the mass transport within the model polymer film [18-22], and predicts the existence

of an overpotential gradient across the width of the model film. In this paper we have undertaken an experimental study of the transport properties of PPP, and will show that the model described in [17] adequately describes the transient current response of an electrode modified with doped PPP.

Experimental Section

CHEMICALS AND REAGENTS

Supporting electrolytes were obtained from various sources. Tetramethylammonium tetrafluoroborate (TMAF), tetraoctylammonium perchlorate (TOAP), tetrapropylammonium perchlorate (TPAP), and tetraethylammonium perchlorate (TEAP) were obtained from Fluka; tetraethylammonium tetrafluoroborate (TEAF) was obtained from Aldrich; lithium tetrafluoroborate was from Alfa; lithium perchlorate was obtained from Smith Chemical, and lithium hexafluoroarsenate came from USS Agrichemicals. Tetrabutylammonium tetrafluoroborate (TBAF) was prepared as previously described [23]. All supporting electrolytes (with the exception of LiAsF_6 , which was "electrochemical grade" and used as received) were recrystallized twice and stored in a vacuum oven at 75° C at least 24 h before use.

Acetonitrile (Baker Chemicals) was HPLC grade (0.001% nominal water content) and was stored over alumina (Woelm Supergrade). All solutions were degassed with dry helium immediately prior to experimentation.

The electrolyte for the silver wire reference electrode was 0.01M silver nitrate with 0.10 M supporting electrolyte in acetonitrile. All potentials are reported vs. the Ag/Ag^+ reference.

ELECTROCHEMISTRY

Electrode potential was controlled via a three electrode potentiostat and waveform generator (JAS Instrument Systems, Inc.). The electrochemical cell contained a 7 mm diameter platinum mirror disk working electrode and a planar platinum foil auxiliary electrode situated opposite the Pt mirror disk. A Luggin reference probe was placed about 1 mm from the working electrode surface. Voltammetric data were recorded on a plotter (Hewlett-Packard 7015B) while chronoamperograms were stored on a digital oscilloscope (Tektronix 5223). Desired signal averaging was computer controlled (IBM PC/AT) as previously described [24].

Electrochemical deposition of poly(paraphenylene) onto the working electrode surface was accomplished by the anodic polymerization of biphenyl (5 mM in 10 mM supporting electrolyte in acetonitrile) while sweeping the potential from 0 to +2.2 V (vs. Ag/Ag⁺) at a desired sweep rate [25]. By careful monitoring of the sweep rate it was possible to control the polymer thickness precisely. PPP films varied in thickness from about 0.2 to 2.0 μm , as computed via the method of Peerce and Bard [26]. When cast electrochemically in this manner, the PPP films were "doped" with supporting electrolyte; the degree of doping varied from one electrolyte to another. Computed concentration of stored charge (a measure of the degree of electrolyte doping) in 1 μm thick films varied from 1.4×10^{-10} moles for LiClO₄/PPP films to 2.6×10^{-8} moles for TOAP/PPP polymers. The films were rinsed with dry acetonitrile, and were characterized by cyclic voltammetry [27] and by chronoamperometry [4, 25] in a solution which contained only the same supporting electrolyte (0.10M in CH₃CN) as was present in the electrodeposition experiment.

Results and Discussion

Poly(paraphenylene) Modified Electrodes

ION STUDIES

The observed deposition currents for films formed in the presence of various supporting electrolytes are shown in Figure 1. Irreversible anodic oxidation of biphenyl results in electrodeposition of doped poly(paraphenylene), and the degree of doping varies depending on the nature of the supporting electrolyte. Polymer film thicknesses were estimated using the method of Peerce and Bard [26]:

$$l = \frac{QM_r}{F\rho A}$$

where l is the thickness of the polymer layer, Q is the quantity of charge passed during electrodeposition, M_r is the molecular weight of the biphenyl repeating unit, F is the Faraday constant, A is the electrode surface area, and ρ is the density of the polymer film (approximately 1 g/cm³). A mean film thickness of approximately 1 μ m was calculated for poly(paraphenylene) deposited at a sweep rate of 25 mV/s.

It is evident from Figure 1(c) that the nature of the supporting electrolyte anion present during electrodeposition has an effect on the behavior of the poly(paraphenylene) film. Differences in supporting electrolyte cations, however, have a smaller effect on the deposition current (Figure 1(a, b)).

The characteristic voltammetry of the doped PPP films under oxidative conditions is shown in Figure 2. In all cases the conducting polymer is in a "neutral" state at 0 V and is "switched on" to an oxidized state at +1V. The voltammetry is reproducible for at least 50 scans. However, the degree of

oxidation (as measured by the peak current on the positive sweep) varies markedly depending on the identity of the dopant anion (Figure 2(c)) as well as cation (Figure 2(a, b)). The effect of the nature of the supporting electrolyte anion has been observed previously in other conductive polymer systems [28, 29]. It is interesting that the size of the supporting electrolyte cation (present during polymer deposition) has such a substantial influence on the film voltammetry under oxidative conditions. These results suggest that the supporting electrolyte cation co-deposits into the polymer matrix along with the anion (but not in 1:1 stoichiometry), and this affects the film transport properties.

The voltammetric results demonstrate that tetrafluoroborate/PPP and hexafluoroarsenate/PPP films (Figure 2(a, c)) are quite capacitative [30], while perchlorate/PPP films show little or no capacitative current (Figure 2(b, c)). Increasing the size of the supporting electrolyte cation from lithium to tetraoctylammonium changes the polymer from primarily an insulating state (for example, $\text{LiClO}_4/\text{PPP}$ and TEAP/PPP polymers) to a highly conducting, oxidized state (e.g., TOAP/PPP). Table 1 lists the calculated number of moles of stored charge (a measure of the degree of doping) in each of the nine doped films studied.

It is also interesting to note the cation size effect which manifests itself in the perchlorate/PPP films. Co-deposition of a large tetraoctylammonium cation into the polymer matrix apparently causes substantial differences in film morphology compared with, say, a tetraethylammonium cation, which is much smaller in size. Although the amount of polymer deposited is the same in both cases (as determined from the number of moles of reacted biphenyl during electrodeposition), the amount of stored charge within the two film types is quite disparate. This was confirmed by an experiment wherein a potential difference of 750 mV between TOAP/PPP and TEAP/PPP modified electrodes was

measured in an electrolyte solution (0.10 M TBAF in CH_3CN). Similar results were obtained for TOAP/PPP films vs. LiClO_4 /PPP polymers, where potential differences of greater than a volt were measured in an electrolyte solution. These observations also demonstrate the possible utility of these p-doped PPP films in battery applications [3, 25, 31-35].

We offer the following suggestions regarding the polymer film morphologies based on the electrochemical data. TOAP/PPP polymers, because of the large co-deposited cation, are swelled compared with TEAP/PPP matrices. This causes a greater degree of porosity in the TOAP-doped films with respect to TEAP-doped PPP. Hence, ion transport by diffusion and migration through the film is enhanced in TOAP/PPP polymers compared with TEAP/PPP films. This is indicated by the greater currents measured in TOAP/PPP vs. TEAP/PPP films (Figure 2(b)). Similar porosity effects have been reported previously for polypyrrole modified electrodes [36]. The above rationale can be extended to explain the voltammetric results obtained for the other doped PPP films studied (Figure 2(a-c)).

The anion effect on film voltammetric behavior is not simply one of anion size (Figure 2(c)), as was originally thought [28]. Morphological properties of these polymer films are obviously dependent upon the doping mechanism during electrodeposition. Studies on the kinetics and mechanisms of film growth in the presence of different dopant anions will become possible with the development of quartz microbalance techniques combined with electrochemical methods. Such microgravimetric methods [37] should prove useful in accounting for the nuances in polymer electrodepositions imparted by anions of varying nature (e.g., size, acidity, nucleophilicity, etc.), since electrochemical methods alone are not useful for describing the kinetic and mechanistic aspects of all facets of the electrodeposition process, which is extremely complicated. Fast transient

spectroelectrochemical experiments might also provide some clues to this question.

A proposed mechanism for the electrodeposition of poly(paraphenylene) is outlined in Scheme 1.

(Scheme 1)

Anodic oxidation of neutral biphenyl is initiated electrochemically, and subsequent radical-radical coupling reactions between monomer and oligomer radicals result in film growth. A similar mechanism has been proposed to describe the electrodeposition of poly(pyrrole) [38]. The precise role which the supporting electrolyte plays during electrodeposition is at this point unclear.

In an effort to more closely study the transport properties of the doped PPP films, large potential step chronoamperometric experiments were carried out; the results are shown in Figure 3. In both tetrafluoroborate- and perchlorate-doped polymers there is a straightforward trend of greater measured overall flux with increased cation size (Figure 3(a, b)). Again, these observations can be explained in terms of a greater degree of porosity within the polymer matrix as cation size is increased. As the film becomes charged (oxidized) during the applied anodic pulse, anions are able to percolate faster through a more porous matrix than through a more compact one. Therefore a polymer matrix which is highly swollen (i.e., has a large mean pore size) can be electrochemically converted more rapidly than a compact polymer. This phenomenon follows from theoretical predictions; for example, see the current- and conversion-distance profiles shown in ref. [17].

An interesting chronoamperometric result which is worthy of note is obtained

from a TOAP/PPP modified electrode (Figure 3(b)), where there is a pronounced shoulder, followed by a decay of current with time. Similar chronoamperometry has been observed previously in poly(vinylferrocene) [4] and other polymer modified electrode systems. Such features were predicted theoretically in the model previously outlined (Figure 4, ref. [17]). At short times the effects of mass transport near the polymer/solution interface have not yet reached the region inside the polymer matrix. At long times, when the bulk of the film has been converted, the current decays exponentially [15].

Chronoamperometric results for polymers doped with various anions are shown in Figure 3(c). Lithium hexafluoroarsenate/poly-(paraphenylene) gives rise to a faster current decay than lithium tetrafluoroborate/PPP during an applied potential step. This observation stands in contrast with what would be expected if anion size were the primary criterion upon which the rate of ion diffusion through the polymer was based. In this case the larger anion (AsF_6^-) relates to a higher γ (diffuso-kinetic parameter) value than does the smaller moiety (BF_4^-) (see Figure 4(a), ref. [17]). This result might possibly be explained in terms of differences in the magnitude of the variable C (Figure 4(b), ref. [17]); however, the voltammetric data (Figure 2(c)), which give comparable measures of film electroactivity (meaning that concentrations of anion and PPP(+) within the different polymer matrices are comparable), rule out this possibility. Obviously there are morphological differences established during polymer electrodeposition which are caused by differences in the nature of the supporting electrolyte anion. Interactions such as ion pairing may play a substantial role in determining the film characteristics.

Lithium perchlorate/PPP polymers are for the most part electroinactive (Figures 2(c), 3(c)); most of the measured current can be assigned to

capacitative charging. These results are similar to those obtained from $\text{LiClO}_4/\text{PPP}$ films prepared by electrodeposition from benzene in HF [31]. The reasons for the observed differences in film characteristics from one $\text{Li}^+\text{anion}^-/\text{PPP}$ polymer to another are at this point unclear.

Experimental current vs. $1/\sqrt{t}$ plots for the above doped polyparaphenylene electrodes are shown in Figure 4. The effects of slow mass transfer of ions through the films are evident from the observed deviations from behavior which would be expected for diffusion in a semi-infinite medium (i.e., "ideal" behavior). Take, for example, the $i-\sqrt{t}$ plot for TOAP/PPP polymer (Figure 4(b)). Contributions of migration and slow diffusion through the film give rise to the "hump" which is observed at intermediate times. This feature was predicted theoretically by the model presented previously (Figure 5, ref. [17]).

Chronocoulometric plots for the nine films studied are shown in Figure 5. Again, we see significant deviations from behavior which would be expected for the "ideal" case of diffusion alone in a semi-infinite medium: charge vs. $1/\sqrt{t}$ plots are nonlinear in all but one case. The nearly linear Q vs. t experimental behavior at short times approximates the theoretical predictions (Figure 6, ref. [17]) for some of these films. Comparison between simulation and experiment is especially good for the case of TOAP/PPP films (Figure 6), where the contribution of capacitative current to the overall current is negligible.

Film Thickness Studies

The chronoamperometry and current vs. $1/\sqrt{t}$ behavior for TBAF/PPP films of varying thickness are shown in Figure 7. The experimental results follow in a straightforward manner what was theoretically predicted in ref. [17]: mass transport through the polymer layer is faster in thin films than in thick ones.

Note the similarities between the model simulations (Figures 4(a) and 5(a) of ref. [17]) and the experimental data (Figure 7). The diffusio-kinetic parameter γ would be expected to have a higher value in a thin film than in a thick layer, assuming no change in the magnitude of the variable C . This is indeed the case experimentally; concentrations of PPP(+) and dopant anion within the polymer matrix do not vary appreciably with differences in film thickness (i.e., the polymer films are quite homogeneous). Similar results were obtained from PPP films of varying thickness electrodeposited in the presence of the other supporting electrolytes utilized in this study.

Film Charge/Discharge Behavior

In an effort to examine the discharge characteristics of doped PPP-modified electrodes a double potential step chronoamperogram was obtained from a very thick ($>5\mu\text{m}$) TOAP/PPP film (Figure 8). Large plateau currents are observed at short times during both the "on" pulse and "off" pulse. Film discharge is extremely slow, as evidenced by the slow decay of current toward baseline (following the current plateau at short times). The observed quasi-reversible behavior is characteristic of many organic conducting polymer systems.

Inclusion of Double Layer Charging and Capacitative Currents in Simulated Chronoamperograms

High capacitances in conductive polymer systems have often been attributed to the large surface areas of the polymers, which enable ion insertion [39]. It has been suggested that these high capacitances are not simply due to double layer charging, a quantity which is much smaller in magnitude [40]. Nonetheless, the total capacitative current must make appreciable contribution to the overall

measured current. The effects of such capacitative currents on the simulated transients such as those depicted in ref. [17], can be estimated in an approximate way using a simple model. Interfaces in close contact with bulk electrolyte will show a normal RC charging behavior indicated by i_{dl} in Figure 9. We make the simplest possible assumption about the charging of the polymer matrix, namely, that the capacitative current is constant with time. Figure 9(b) shows the overall current which would be measured if the illustrated contributions due to charging and capacitative currents were added to the Faradaic current component. Double layer charging currents should not vary considerably from one doped polymer to another, but variations in conductive polymer capacitance can be significant, depending on the dopant. Recall that tetrafluoroborate/ PPP and hexafluoroarsenate/PPP polymers demonstrated capacitative behavior, while perchlorate-doped PPP films did not exhibit appreciable capacitative currents. Figure 9(b) shows the simulated current-time transient for a γ value of 10.0 and a C value of 0.5. By increasing the value of γ , simulated transients which approximated experimental TBAF/PPP chronoamperometric behavior were obtained (Figures 10 and 11). Similarly, Yap and Durst [16] included double layer and capacitative contributions in their model, and obtained good agreement between simulated and experimental current transients for an inorganic conducting polymer film.

Conclusion

In this paper chronoamperometric results demonstrate the applicability of the macroscopic transport model described previously [17]. Contributions of diffusion, migration, double layer charging, and polymer capacitance have been considered in simulating experimental current-time profiles. Experimental

chronoamperometric results from doped PPP modified electrodes compare favorably with simulated current transients. It is suggested that the basis of the previously proposed model can be extended to apply to other conductive polymer systems, special cases being developed from the general model

The experiments reported here show that it is not possible to derive full descriptions of the system from the electrochemical experiments alone. The combination of conventional electrochemical experiments with fast spectroelectrochemical measurements would undoubtedly provide additional useful information e.g. as to the nature and concentration of the incorporated ions. We note that such information could also be derived by the combination of electrochemical and quartz microbalance techniques (37).

Acknowledgment

We thank the Office of Naval Research for support of this work.

References

1. Bredas, J. L.; Street, G. B. Acc. Chem. Res. 1985, 18, 309.
2. Kaufman, J. H. Ph.D. Thesis, University of California, Santa Barbara, Calif. USA, 1984.
3. Frommer, J. E.; Chance, R. R. in Encyclopedia of Polymer Science and Engineering, Vol. 5, 2nd Ed. Wiley: New York, 1986.
4. Bandyopadhyay, S. Ph.D. Thesis, University of Utah, Salt Lake City, UT, USA, 1985.
5. Duke, C. B.; Meyer, R. J. Phys. Rev. B 1981, 23, 211.
6. Kaufman, F. B.; Engler, E. M. J. Am. Chem. Soc. 1979, 101, 547.
7. Murray, R. W. in Electroanalytical Chemistry, Vol. 13. Bard, A. J., Ed. Marcel Dekker: New York, 1984.
8. White, H. S.; Leddy, J.; Bard, A. J. J. Am. Chem. Soc. 1982, 104, 4811.
9. Chambers, J. Q.; Kaufman, F. B.; Nichols, K. H. J. Electroanal. Chem. 1982, 147, 277.
10. Anson, F. C.; Saveant, J. M.; Shigehara, K. J. Am. Chem. Soc. 1983, 105, 1096.
11. Andrieux, C. P.; Hapiot, P.; Saveant, J. M. J. Electroanal. Chem. 1984, 172, 49.
12. Tsou, Y. M.; Anson, F. C. J. Phys. Chem. 1985, 89, 3818.
13. Elliot, C. M.; Redepenning, J. G. J. Electroanal. Chem. 1984, 181, 137.
14. Pickup, P. G.; Osteryoung, R. A. J. Electroanal. Chem. 1985, 186, 99.
15. Yap, W. T.; Durst, R. A.; Blubaugh, E. A.; Blubaugh, D. D. J. Electroanal. Chem. 1983, 144, 69.
16. Yap, W. T.; Durst, R. A. J. Electroanal. Chem. 1987, 216, 11.
17. Ashley, K.; Pons, S.; Fleischmann, M. This Journal, p. ?. (Modelling, Part I)
18. Newman, J. S.; Tobias, C. W. J. Electrochem. Soc. 1962, 109, 1183.
19. Rousar, I.; Micka, K.; Kimla, A. Electrochemical Engineering, Vol. 21B; Elsevier: Amsterdam, 1986, Part E.
20. Simmonson, D. J. Appl. Electrochem. 1973, 3, 261.

21. Newman, J.; Tiedemann, W. A. I. Ch. E. J. 1975, 21, 25.
22. Oliver, S. F. Ph.D. Thesis, The University, Southampton, UK, 1983.
23. Clark, D. B.; Fleischmann, M.; Pletcher, D. J. Chem. Soc., Perkin Trans. II 1973, 1578.
24. Ashley, K.; Foley, J. K.; Mei, Q.; Ghoroghchian, J.; Sarfarazi, F.; Cassidy, J.; Halton, B.; Stang, P. J.; Pons, S. J. Org. Chem. 1986, 51, 2089.
25. McAleer, J. F.; Ashley, K.; Smith, J. J.; Bandyopadhyay, S.; Ghoroghchian, J.; Eyring, E. M.; Pons, S.; Mark, H. B. J. Mol. Electron. 1986, 2, 183.
26. Pearce, P. J.; Bard, A. J. J. Electroanal. Chem. 1980, 114, 97.
27. Josowicz, M.; Janata, J.; Ashley, K.; Pons, S. Anal. Chem. 1987, 59, 253.
28. Armand, M. B.; Chabagno, J. M.; Duclot, M. J. in Fast Ion Transport in Solids; Vashishta, P.; Mundy, J. N.; Shenoy, G. K.; Eds. Elsevier North Holland: Amsterdam, 1979, p. 131.
29. Diaz, A.; Castillo, J. I.; Logan, J. A.; Lee, W. Y. J. Electroanal. Chem. 1981, 129, 115.
30. Feldberg, S. W. J. Am. Chem. Soc. 1984, 106, 4671.
31. Rubinstein, I. J. Polym. Sci. 1983, 21, 3035.
32. Rubinstein, I. J. Electrochem. Soc. 1983, 130, 1506.
33. Satoh, M.; Tabata, M.; Kaneto, K.; Yoshino, K. Jpn. J. Appl. Phys., Part 2 1986, 25, L73.
34. Satoh, M.; Tabata, M.; Kaneto, K.; Yoshino, K. J. Electroanal. Chem. 1985, 195, 203.
35. Tabata, M.; Satoh, M.; Kaneta, K.; Katsumi, Y. J. Phys. C: Solid State Phys. 1986, 19, L101.
36. Skotheim, T. A.; Feldberg, S. W.; Armand, M. B. J. Phys. (Paris) 1983, 44, 44.
37. Buttry, D.; Orata, D.; Varineau, P.; Wen, T. C. Paper presented at 193rd National Meeting, American Chemical Society, Denver (1987).
38. Genies, E. M.; Bidan, G.; Diaz, A. F. J. Electroanal. Chem. 1983, 149, 1.
39. Jow, T. R.; Jen, K. Y.; Elsenbaumer, R. L.; Shacklette, L. W.; Angelopoulos, M.; Cava, M. Synth. Met. 1986, 14, 53.
40. Jow, T. R.; Shacklette, L. W. Abstr. 620, 166th Meeting, The Electrochemical Society, New Orleans (1984).

<u>Dopant</u>		<u># moles of charge</u>
perchlorate electrolytes	TOAP	2.6×10^{-9}
	TPAP	1.9×10^{-9}
	TEAP	4.0×10^{-10}
tetrafluoroborate electrolytes	TBAF	3.2×10^{-9}
	TEAF	2.6×10^{-9}
	TMAF	2.1×10^{-9}
lithium electrolytes	LiAsF ₆	4.6×10^{-10}
	LiBF ₄	5.9×10^{-10}
	LiClO ₄	1.4×10^{-10}

Table 1. Moles of charge stored in 7mm \times 1 μ m doped PPP films.

Figure Legends

- Figure 1. Cyclic voltammograms recorded at a Pt disk electrode in 5 mM biphenyl solution with 10 mM supporting electrolyte (indicated) in CH_3CN ; sweep rate is 25 mV/s.
- Figure 2. Cyclic voltammograms recorded from approx. 1 micron thick poly(paraphenylene) modified electrodes in 0.10 M supporting electrolyte (indicated) in CH_3CN ; sweep rate is 100 mV/s.
- Figure 3. Chronoamperograms recorded from approx. 1 micron thick doped PPP-modified electrodes in 0.10 M supporting electrolyte (indicated) in CH_3CN . Potential step is $0 \rightarrow +1.0\text{V}$ vs. Ag/Ag^+ .
- Figure 4. Cottrell plots from approx. 1 micron thick doped PPP electrodes. Conditions same as in Figure 3.
- Figure 5. Chronocoulometric plots from approx. 1 micron thick doped PPP films. Conditions same as in Figure 3.
- Figure 6. Charge vs. $t^{-1/2}$ plots: — simulation ($\gamma = 10.0$, $C = 0.7$ (see ref. [17] for explanation of parameters)); • experimental data from approx. 1 micron thick TOAP/PPP film.
- Figure 7. (a) Chronoamperometric and (b) current vs. $t^{-1/2}$ data from TBAF/PPP films of varying thickness: --- 1.4 micron; — 1 micron; ---- 0.5 micron. Experimental parameters same as in Figure 3.
- Figure 8. Double potential step chronocoulometry of very thick (approx. 10 microns) TOAP/PPP film; potential step $0 \rightarrow +1.0\text{ V}$ vs. Ag/Ag^+ of 500 ms duration. Other parameters same as in Figure 3.
- Figure 9. Illustration of (a) contributions of charging (i_{dl}) and capacitive (i_c) currents to the overall "measured" current in a simulated chronoamperogram. Simulated Faradaic current (i_f) is predicted theoretically using $\gamma = 10$, $C = 0.5$. (b) The sum of the contributions in (a).
- Figure 10. Simulated current transient (•) vs. experimental i - t plot (—). For the simulation we have used $\gamma = 100$, $C = 0.5$, $i_c = 1$, and $i_{dl} = \exp[-1/t]$ (dimensionless)]. Other parameters same as in Figure 3.
- Figure 11. Simulated (x) i vs. $t^{-1/2}$ (dimensionless) plot vs. experimental (o) i vs. $t^{-1/2}$ data. Parameters same as in Figure 10.

TECHNICAL REPORT DISTRIBUTION LIST, GEN

	<u>No. Copies</u>		<u>No. Copies</u>
Office of Naval Research Attn: Code 1113 800 N. Quincy Street Arlington, Virginia 22217-5000	2	Dr. David Young Code 334 NORDA NSTL, Mississippi 39529	1
Dr. Bernard Douda Naval Weapons Support Center Code 50C Crane, Indiana 47522-5050	1	Naval Weapons Center Attn: Dr. Ron Atkins Chemistry Division China Lake, California 93555	1
Naval Civil Engineering Laboratory Attn: Dr. R. W. Drisko, Code L52 Port Hueneme, California 93401	1	Scientific Advisor Commandant of the Marine Corps Code RD-1 Washington, D.C. 20380	1
Defense Technical Information Center Building 5, Cameron Station Alexandria, Virginia 22314	12 high quality	U.S. Army Research Office Attn: CRD-AA-IP P.O. Box 12211 Research Triangle Park, NC 27709	1
DTNSRDC Attn: Dr. H. Singerman Applied Chemistry Division Annapolis, Maryland 21401	1	Mr. John Boyle Materials Branch Naval Ship Engineering Center Philadelphia, Pennsylvania 19112	1
Dr. William Tolles Superintendent Chemistry Division, Code 6100 Naval Research Laboratory Washington, D.C. 20375-5000	1	Naval Ocean Systems Center Attn: Dr. S. Yamamoto Marine Sciences Division San Diego, California 91232	1

ABSTRACTS DISTRIBUTION LIST, SDIO/IST

Dr. Robert A. Osteryoung
Department of Chemistry
State University of New York
Buffalo, NY 14214

Dr. Douglas N. Bennion
Department of Chemical Engineering
Brigham Young University
Provo, UT 84602

Dr. Stanley Pons
Department of Chemistry
University of Utah
Salt Lake City, UT 84112

Dr. H. V. Venkatesetty
Honeywell, Inc.
10701 Lyndale Avenue South
Bloomington, MN 55420

Dr. J. Foos
EIC Labs Inc.
111 Downey St.
Norwood, MA 02062

Dr. Neill Weber
Ceramatec, Inc.
163 West 1700 South
Salt Lake City, UT 84115

Dr. Subhash C. Narang
SRI International
333 Ravenswood Ave.
Menlo Park, CA 94025

Dr. J. Paul Pemsler
Castle Technology Corporation
52 Dragon Ct.
Woburn, MA 01801

Dr. R. David Rauh
EIC Laboratory Inc.
111 Downey Street
Norwood, MA 02062

Dr. Joseph S. Foos
EIC Laboratories, Inc.
111 Downey Street
Norwood, Massachusetts 02062

Dr. Donald M. Schleich
Department of Chemistry
Polytechnic Institute of New York
333 Jay Street
Brooklyn, New York 01

Dr. Stan Szpak
Code 633
Naval Ocean Systems Center
San Diego, CA 92152-5000

Dr. George Blomgren
Battery Products Division
Union Carbide Corporation
25225 Detroit Rd.
Westlake, OH 44145

Dr. Ernest Yeager
Case Center for Electrochemical
Science
Case Western Reserve University
Cleveland, OH 44106

Dr. Mel Miles
Code 3852
Naval Weapons Center
China Lake, CA 93555

Dr. Ashok V. Joshi
Ceramatec, Inc.
2425 South 900 West
Salt Lake City, Utah 84119

Dr. W. Anderson
Department of Electrical &
Computer Engineering
SUNY - Buffalo
Amherst, Massachusetts 14260

Dr. M. L. Gopikanth
Chemtech Systems, Inc.
P.O. Box 1067
Burlington, MA 01803

Dr. H. F. Gibbard
Power Conversion, Inc.
495 Boulevard
Elmwood Park, New Jersey 07407

DL/1113/87/2

ABSTRACTS DISTRIBUTION LIST, SDIO/IST

Dr. V. R. Koch
Covalent Associates
52 Dragon Court
Woburn, MA 01801

Dr. Randall B. Olsen
Chronos Research Laboratories, Inc.
4186 Sorrento Valley Blvd.
Suite H
San Diego, CA 92121

Dr. Alan Hooper
Applied Electrochemistry Centre
Harwell Laboratory
Oxfordshire, OX11 0RA UK

Dr. John S. Wilkes
Department of the Air Force
The Frank J. Seiler Research Lab.
United States Air Force Academy
Colorado Springs, CO 80840-6528

Dr. Gary Bullard
Pinnacle Research Institute, Inc.
10432 N. Tantan Avenue
Cupertino, CA 95014

Dr. J. O'M. Bockris
Ementech, Inc.
Route 5, Box 946
College Station, TX 77840

Dr. Michael Binder
Electrochemical Research Branch
Power Sources Division
U.S. Army Laboratory Command
Fort Monmouth, New Jersey 07703-5000

Professor Martin Fleischmann
Department of Chemistry
University of Southampton
Southampton, Hants, SO9 5NH UK